Progress In Electromagnetics Research M, Vol. 91, 39–48, 2020

Exact Non-Reflecting Boundary Conditions with an FDTD Scheme for the Scalar Wave Equation in Waveguide Problems

Wim A. Mulder[1, 2, *]

Abstract—Modeling wave propagation often requires a truncation of the computational domain to a smaller subdomain to keep computational cost reasonable. The mere volume of papers on absorbing boundary conditions indicates that a perfect solution is not available. A method is proposed that is numerically exact, at least in the case of a time-domain finite-difference scheme for the scalar wave equation. The word 'exact' is used in the sense that there is no difference between a computation on the truncated domain with this method and one on an enlarged domain with reflecting boundaries that are placed so far away that their reflections cannot reach the original domain within the modeled time span. Numerical tests in 1D produce stable results with central difference schemes from order 2 to 24 for the spatial discretization. The difference with a reference solution computed on an enlarged domain with the boundary moved sufficiently far away only contains accumulated numerical round-off errors. Generalization to more than one space dimension is feasible if there is a single non-reflecting boundary on one side of a rectangular domain or two non-reflecting boundaries at opposing sides, but not for a corner connecting non-reflecting boundaries. The reason is that the method involves recursion based on translation invariance in the direction perpendicular to the boundary, which does not hold in the last case. This limits the applicability of the method to, for instance, modeling waveguides, or exactness has to be partially given up.

1. INTRODUCTION

The numerical simulation of wave propagation on infinite domains often requires truncation to a domain of finite size to make the computation tractable. This leads to non-physical boundary conditions that go by names like artificial, absorbing, transparent, transmitting, radiation, open, or non-reflecting. The vast body of literature on the subject indicates that this is not an easy problem. For references, the reader is referred to one or more of several review and comparison articles [1–7].

The focus of this paper is on exact boundary conditions. The name 'perfectly matched layer' (PML) [8] suggests that these already exist. However, this type of boundary condition requires damping or absorption. The problem with a damping layer is that it produces reflections, similar to and sometimes indistinguishable from a variation in wave speed [9]. As a result, this type of boundary cannot be perfect. Another type of exact boundary condition is based on Green's second identity [10], but has a long-term instability that can be repaired by adding some dissipation to the time stepping scheme [11]. An alternative is a boundary integral formulation [12].

In this paper, 'exact' is used in a different sense: the difference between the numerical solution on the truncated domain and on an infinite domain should be zero. In practice, the infinite domain will be finite but large enough to prevent the reflections from the boundary to reach the truncated domain. In addition, the difference will not be zero but equal to the accumulated numerical round-off errors. To extend a wave speed model given in the original truncated domain into the enlarged domain, piecewise

Received 12 December 2019, Accepted 31 March 2020, Scheduled 4 April 2020

* Corresponding author: W. A. Mulder (wim.mulder@shell.com).

[1] Shell Global Solutions International BV, Amsterdam, The Netherlands. [2] Delft University of Technology, Delft, The Netherlands.

constant extrapolation of the value on the boundary is assumed in 1D. In more than one dimension, this extrapolation is accomplished in the direction perpendicular to the boundary. When carried out sequentially per coordinate, corners are handled automatically.

Numerical exactness is in fact overdone. It is sufficient if spurious reflections generated by an imperfect boundary are much smaller in amplitude than the numerical errors produced by the spatial and temporal discretization of the interior scheme. Usually, one of the classic absorbing boundary conditions [13–15] in combination with a carefully tuned PML strip [8, 16] will provide satisfactory results. In some cases, when studying very weak reflections in the presence of strong incoming waves, this careful tuning may be cumbersome and the proposed boundary condition can offer an alternative.

The exposition in the next section alternates between an explanation of the method and an illustrative example. It starts with a description of the proposed exact method for the lowest-order time-domain finite-difference approximation of the scalar wave equation in one space dimension. This is followed by its generalization to higher-order spatial schemes. Then, the lowest-order 2-D case on a rectangular domain with three reflecting and one non-reflecting boundary condition is considered. This requires a further generalization of the method. Finally, a rectangular domain with two adjacent non-reflecting boundaries is examined. At that point, the generalization fails. The section ends with estimates of the method's computational complexity. The last section summarizes the main conclusions.

2. METHOD AND EXAMPLES

2.1. 1D, Second Order

The scalar wave equation reads

$$\frac{1}{c^2}\frac{\partial^2 u}{\partial t^2} = \frac{\partial^2 u}{\partial x^2} + f. \tag{1}$$

The solution $u(t,x)$ depends on time t and position x. The wave speed $c(x)$ may vary over the domain. The forcing function $f(t,x)$ injects a signal into the computational domain. An example is a point source at position x_s with source signature $w(t)$, represented by $f(t,x) = w(t)\delta(x - x_s)$.

For the finite-difference discretization, a grid on the domain $[x_{\min}, x_{\max}]$ with N points is defined by $x_i = x_{\min} + (i - \frac{1}{2})\Delta x$, $i = 1, \ldots, N$, $\Delta x = (x_{\max} - x_{\min})/N$. The boundary condition at the left, at $x_{\min}$, is taken as zero Neumann, and the one at the right, at $x_{\max}$, should be non-reflecting. The standard second-order finite-difference scheme in space and time is given by

$$\frac{1}{c_i^2 \Delta t^2}\left(u_i^{n+1} - 2u_i^n + u_i^{n-1}\right) = \frac{1}{\Delta x^2}\left(u_{i+1}^n - 2u_i^n + u_{i-1}^n\right) + f_i^n, \tag{2}$$

where time is discretized as $t_n = t_0 + n\Delta t$. The wave speed $c_i = c(x_i)$. The discrete solution is $u_i^n = u(t_n, x_i)$ and runs up to some value $t_{\max} = t_0 + N_t \Delta t$. An optional forcing function is denoted by $f_i^n = f(t_n, x_i)$. The time step Δt should obey $c_{\max}\Delta t/\Delta x \le 1$ for stability, with $c_{\max} = \max_i c_i$. A zero Neumann boundary condition can be imposed by symmetric mirroring, letting $u_0 = u_1$, and a zero Dirichlet boundary condition by anti-symmetric mirroring with $u_0 = -u_1$.

Consider the boundary on the right with the interior grid point x_N next to it. To avoid reflections, we can extend the domain to the right with the wave speed c_N at the last grid point. If the boundary is moved sufficiently far away, its reflections will not be able to reach x_N. Note that the numerical wave speed for a second-order scheme is one grid spacing Δx per time step, so an extension with a size of at least $N_a = \frac{1}{2}(t_{\max} - t_0)/\Delta t$ grid points will do, resulting in a grid with $N_e = N + N_a$ points.

We can try to reduce the cost of the enlarged domain by 'learning'. Consider the grid point at x_N and define a unit spike in the original, interior domain:

$$v_i^n = \delta_{i,N}\delta_{n,0}, \quad 1 \le i \le N, \tag{3}$$

where the Kronecker delta is used. Here, the symbol v replaces u to avoid confusion further on. The discrete time stepping scheme in the exterior domain provides

$$v_i^{n+1} = 2v_i^n - v_i^{n-1} + \sigma\left(v_{i+1}^n - 2v_i^n + v_{i-1}^n\right), \quad i > N, \tag{4}$$

with $\sigma = (c_N \Delta t/\Delta x)^2$. The wave speed should be set to c_N in the enlarged domain, with $i = N+1, \ldots, N_e$. We then start time stepping from the initial values at $n = -1$ and $n = 0$ on the

full domain, setting $v_i^n = 0$, for all $1 \le i \le N$ and $n > 0$ after each time step. In that case, the wave speed in the interior can also be set to c_N, as long as Δt is not changed. Alternatively, we can perform the time steps of Equation (4) in the exterior domain only, using the unit spike as a boundary value. The values of the boundary Green function at $i = N + 1$ can be recorded and used to predict those at the point $x_N + \Delta x$ for another problem with solution u_i^n, $i = 1, \ldots, N$, defined in the interior, in the original domain. The recorded values are denoted by $g^n = v_{N+1}^n$ for $n = 1, \ldots, N_t$.

Of course, the computation of g^n in this way is as expensive as finding the solution on an enlarged domain. Below, an alternative approach based on recursion will be presented, but let us first assume that we have g^n available. Given a value u_N^n for the interior problem, we can predict its contribution to future points u_{N+1}^m, $m > n$, just outside the domain by

$$u_{N+1}^m := u_{N+1}^m + g^{m-n} u_N^n, \quad m = n+1, \ldots, N_t. \tag{5}$$

u_{N+1}^n must have been initialized to zero for all $n = 0, \ldots, N_t$. After each update, it can be used in Eq. (2) for the next step. Instead of predicting into the future, we can predict from the past with

$$u_{N+1}^n = \sum_{m=1}^{n} g^m u_N^{n-m} = \sum_{m=0}^{n-1} g^{n-m} u_N^m, \quad n > 0. \tag{6}$$

2.2. Recursion

The computation of g^n can be simplified as follows. We will need two grid points in the exterior next to the boundary, so define an array G_i^n, $i = 1, 2$ and $n = 1, \ldots, N_t$ such that $g^n = G_1^n$. Initialize G_i^0 at $i = 1$ and 2, which correspond to the earlier $N + 1$ and $N + 2$, to zero. Then (4) leads to $G_1^1 = \sigma$ and $G_2^1 = 0$. More precisely, if we set the index for boundary point x_N at $i = 0$ for convenience, then $v_0^0 = 1$ is the unit spike and the other values are zero, providing $v_1^2 = \sigma$ and $v_2^2 = 0$. The next time step produces $G_1^2 = 2(1 - \sigma)G_1^1$ and $G_2^2 = \sigma G_1^1$. Note that we now have a time stepping problem with a constant wave speed and a zero Dirichlet boundary condition at the left. The wave energy spreads to the right at each time step. If we would extend G_i^n to the right, then $G_n^n = \sigma G_{n-1}^{n-1} = \sigma^n$ would be the farthest non-zero solution value at time level $n > 0$. We can truncate the domain, however, by reusing Eq. (6), realizing that not all values are yet available. This step hinges on the fact that the wave speed is assumed to be constant and equal to the value on the boundary in the enlarge domain, that is, $c_i = c_N$ for $i > N$. The result is the recursion

$$G_2^n = \sum_{k=1}^{n-1} G_1^{n-k} G_1^k, \quad n > 1, \tag{7a}$$

$$G_1^n = 2G_1^{n-1} - G_1^{n-2} + \sigma \left(G_2^{n-1} - 2G_1^{n-1} \right), \quad n > 1, \tag{7b}$$

starting from $G_1^0 = 0$, $G_1^1 = \sigma$ and $G_2^1 = 0$. With $g^n = G_1^n$ available, we can apply Equation (5) or (6) in one or more simulations.

2.3. 1-D Example

The method was tested on the dimensionless wave speed model shown in Figure 1(a). The forcing function was a point source $f(t, x) = w(t)\delta(x - x_s)$ at position $x_s = 0.4$ with a source signature $w(t) = 2\frac{\mathrm{d}}{\mathrm{d}t}\left[4\frac{t}{T_w}(1 - \frac{t}{T_w})\right]^{p_w}$ for $0 < t < T_w$ and zero otherwise. Its duration was $T_w = 0.25$ with a power $p_w = 12$. This results into waves proportional to its time integral that travel to the left and right, as shown in Figure 1(b).

The numerical solution at time $t_{\max} = 2$ was compared to one obtained on a much larger domain with a Neumann condition on the right boundary. The grid spacing was $\Delta x = 0.005$ and the time step $\Delta t = 0.004$, at 80% of the maximum value allowed for stability. The observed maximum absolute error of around 3×10^{-14} was caused by accumulated numerical round-off errors, effectively demonstrating the correctness of method and code.

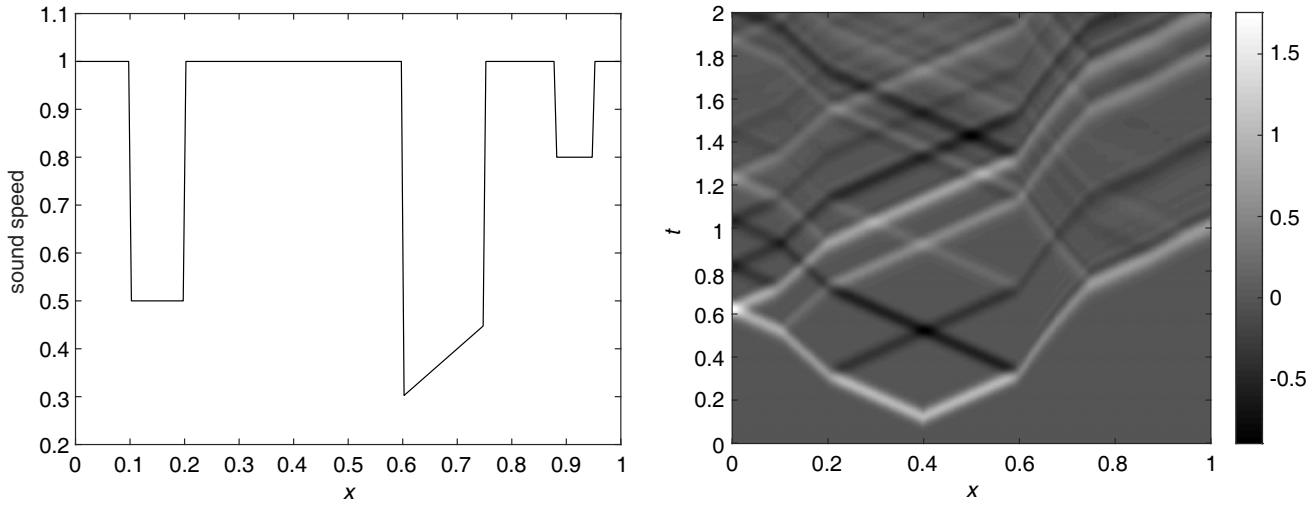

Figure 1. (a) Wave speed model. (b) Time evolution of the wavefield for a point source at $x_s = 0.4$. The Neumann boundary condition at the left generates symmetric reflections. The boundary at the right is perfect.

2.4. 1D, Higher Order

Higher-order schemes are usually more efficient than lower-order schemes, because they require less points per wavelength to reach the same accuracy, which should more than compensate for their higher cost. This is in particular true for smoothly varying wave speed models. If there are many large variations on small length scales, however, the lowest computational cost to reach a given accuracy occurs for lower-order schemes. With large discontinuities in the wave speed, a finite-element method with elements that follow the jumps will be a better choice than a finite differences [17, a.o.], but for now, we stay with the latter.

A finite-difference scheme of higher order M, M even, requires a stencil of $M+1$ points wide. The discrete second derivative $L_i(\mathbf{u})$ at point x_i of the solution represented by the vector $\mathbf{u}$ is given by

$$-\Delta x^2 L_i(\mathbf{u}) = w_0 u_i + \sum_{k=1}^{M/2} w_k (u_{i+k} + u_{i-k}), \tag{8}$$

with weights [17, 18]

$$w_0 = \sum_{j=1}^{M/2} \frac{2}{j^2}, \quad w_k = (-1)^k \sum_{j=k}^{M/2} \frac{2}{j^2} \frac{(j!)^2}{(j-k)!(j+k)!}, \quad k = 1, \ldots, \frac{1}{2}M. \tag{9}$$

Unit spikes now have to be placed at $\frac{1}{2}M$ points $x_{N-(j-1)}$, $j = 1, \ldots, \frac{1}{2}M$: $v_i^n = \delta_{i,\,N-(j-1)} \delta_{n,0}$ for all $1 \le i \le N$ and n. For each $j = 1, \ldots, \frac{1}{2}M$, a separate run on an enlarged domain is required. Because the numerical wave speed is now $\frac{1}{2}M$ points per time step, the number of extra points on the enlarged domain has to be at least $N_a = \frac{1}{4}M(t_{\max} - t_0)$. For each run numbered by j, we can record the values $g_{j,\,m}^n = v_{N+m}^n$, with $m = 1, \ldots, \frac{1}{2}M$.

For another run on the original domain with solution u_i^n, we can then either find the $\frac{1}{2}M$ values just outside the domain by predicting into the future with

$$u_{N+i}^m := u_{N+i}^m + \sum_{j=1}^{M/2} g_{i,j}^{m-n} u_{N-(j-1)}^n, \quad j = 1, \ldots, \frac{1}{2}M, \quad m = n+1, \ldots, N_t, \tag{10}$$

or from the past with

$$u^n_{N+i} = \sum_{m=1}^{n} \sum_{j=1}^{M/2} g^m_{i,j} u^{n-m}_{N-(j-1)}, \quad i = 1, \ldots, \frac{1}{2}M, \quad n > 0. \tag{11}$$

With these extra values, u^n_{N+i}, the second derivatives can be computed up to the last interior point at N.

Instead of modeling on an enlarged domain, recursion can be applied to find $g^n_{i,j}$. The initialization at the first time level, $n = 1$, is given in terms of the finite-difference weights by

$$g^1_{i,j} = -\sigma w_{i+j-1}, \quad i + j \leq 1 + \frac{1}{2}M, \quad i = 1, \ldots, M, \quad j = 1, \ldots, \frac{1}{2}M, \tag{12a}$$

and zero otherwise. Note that the stability limit for σ depends on the order of the scheme [17]. For the subsequent time levels ($n > 1$), the discrete partial differential equation can be used for $i = 1, \ldots, \frac{1}{2}M$. Defining $v_i = g^{n-1}_{i,j}$ for $i = 1, \ldots, M$ and assuming $g^0_{i,j} = 0$ and $v_i = 0$ for $i < 1$, we have

$$g^n_{i,j} = 2g^{n-1}_{i,j} - g^{n-2}_{i,j} + \sigma L_i(\mathbf{v}), \quad i = 1, \ldots, \frac{1}{2}M. \tag{12b}$$

The values for $i = \frac{1}{2}M + 1, \ldots, M$ can be obtained by recursion:

$$g^n_{\frac{1}{2}M+i,\,j} = \sum_{m=1}^{n-1} \sum_{k=1}^{M/2} g^{n-m}_{i,\,\frac{1}{2}M-(k-1)} g^m_{k,\,j}. \tag{12c}$$

Note that the wave speed c_i has to be constant in the last $\frac{1}{2}M$ points for this to work, that is, $c_{N-i} = c_N$ for $i = 0, \ldots, \frac{1}{2}M - 1$. If not, an extra buffer zone of width $\frac{1}{2}M - 1$ with constant wave speed $c(x_N)$ can be added.

The above was verified with the same example as before for orders $M = 2$ to $M = 24$, running at 50% of the order-dependent maximum allowable time step. Again, the difference with a simulation on the enlarged domain was determined by accumulated round-off errors. Figure 2 displays the wavefield with non-reflecting boundaries at both sides, using a spatial discretization of order 24. Note how numerical round-off errors slowly accumulate as time increases in this double-precision computation.

No stability problems of the kind reported by [11] were observed when $t_{\max}$ was increased from 2 to 20 for all orders from 2 to 24.

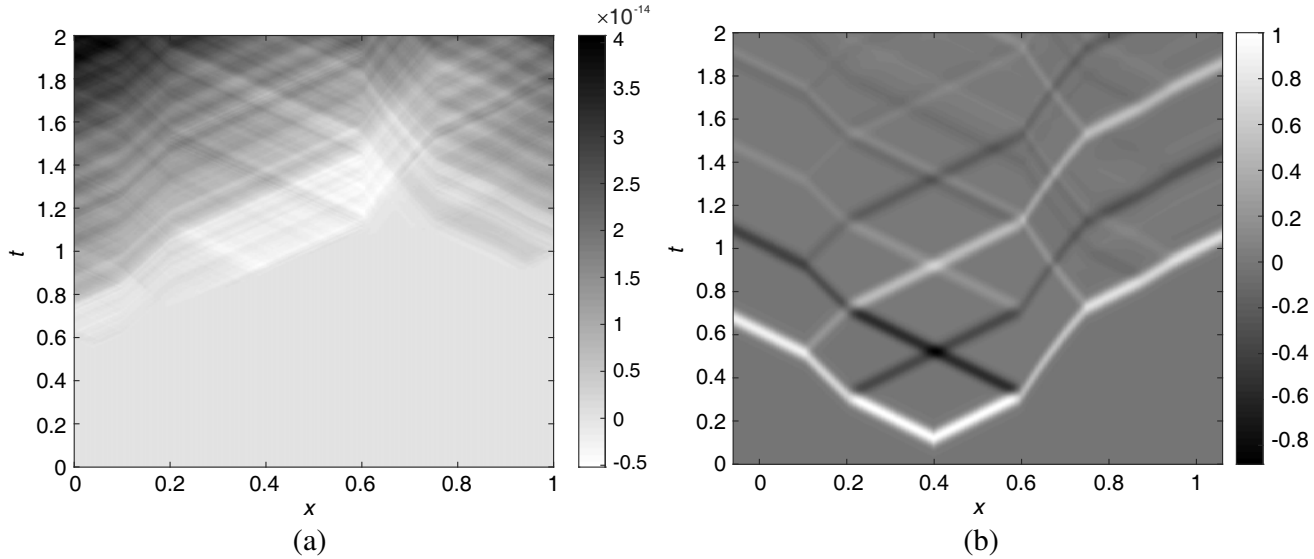

Figure 2. (a) Time evolution of the wavefield for a point source at $x_s = 0.4$ with non-reflecting boundaries at the left and right of the domain and with a 24th-order scheme in space. (b) Difference with a solution computed on an enlarged domain, consisting in accumulated numerical round-off errors.

2.5. 2D, Second Order, One Side

For the generalization to more than one space dimension, we first consider the 2-D case with a finite-difference scheme of lowest order. As a start, a rectangular domain with only one non-reflecting boundary is considered.

The 2-D domain has $x \in [x_{\min}, x_{\max}]$ and $y \in [y_{\min}, y_{\max}]$. Neumann boundary conditions are imposed at all sides except at $x = x_{\max}$. The domain is discretized on a grid with $N_x \times N_y$ points and spacings $\Delta x = (x_{\max} - x_{\min})/N_x$ and $\Delta y = (y_{\max} - y_{\min})/N_y$ in the x- and y-coordinates, respectively. With that, the grid points are $x_i = x_{\min} + i(\Delta x - \frac{1}{2})$ for $i = 1, \ldots, N_x$ and $y_j = y_{\min} + j(\Delta y - \frac{1}{2})$ for $j = 1, \ldots, N_y$.

The discrete time stepping scheme in 2D is

$$u^{n+1}_{i,\,j} = 2u^n_{i,\,j} - u^{n-1}_{i,\,j} + (c_{i,\,j}\Delta t)^2 \left(\frac{u^n_{i+1,\,j} - 2u^n_{i,\,j} + u^n_{i-1,\,j}}{\Delta x^2} + \frac{u^n_{i,\,j+1} - 2u^n_{i,\,j} + u^n_{i,\,j-1}}{\Delta y^2} + f^n_{i,j} \right). \tag{13}$$

The scheme is stable for $c\Delta t\sqrt{\Delta x^{-2} + \Delta y^{-2}} \leq 1$.

As in the 1-D case, the response of a unit spike on the boundary at x_{N_x} can be computed, but now for different y_{j_0}, $j_0 = 1, \ldots, N_y$. For each j_0, let $v^n_{i,j} = \delta_{i,\,N_x}\delta_{j,\,j_0}\delta_{n,0}$ and consider the initial/boundary value problem in the domain extended to right, with $i = N_x + 1, \ldots, N_e$ and N_e sufficiently large to avoid reflections from x_{N_e} returning to $x_{N_x} + \Delta x$. For each $j_0 = 1, \ldots, N_y$, this defines a set of discrete solutions in space and time denoted by $G^n_{i,j;\,N_x,\,j_0} = v^n_{i,j}$, in the enlarged domain $[x_{\min}, x_{N_e}] \times [y_{\min}, y_{\max}]$, or actually $[x_{\max}, x_{N_e}] \times [y_{\min}, y_{\max}]$.

We select a subset $g^n_{j;\,j_0} = G^n_{N_x+1,\,j;\,N_x,\,j_0}$, with $n > 0$ and $j = 1, \ldots, N_y$, from the first point in the enlarged domain. Prediction into the future now involves an additional summation over j_0:

$$u^k_{N_x+1,\,j} := u^k_{N_x+1,\,j} + \sum_{j_0=1}^{N_y} g^{k-n}_{j;\,j_0} u^n_{N_x,\,j_0}, \quad k = n+1, \ldots, N_t. \tag{14}$$

Here, $u^n_{N_x+1,j}$ must have been initialized to zero for all $n = 0, \ldots, N_t$, and the updated values can be used in Eq. (13) for the next time step at t_{n+1}. Alternatively, prediction from the past lets

$$u^n_{N_x+1,\,j} = \sum_{m=1}^{n} \sum_{j_0=1}^{N_y} g^m_{j;\,j_0}\, u^{n-m}_{N_x,\,j_0}. \tag{15}$$

For the expressions based on recursion, it is convenient to define $\sigma^x_j = (c_{N_x,\,j}\Delta t/\Delta x)^2$ and $\sigma^y_j = (c_{N_x,\,j}\Delta t/\Delta y)^2$. The wave speed in the exterior is assumed to be obtained by piecewise constant extrapolation from the boundary values in the direction perpendicular to the boundary, letting $c_{i,j} = c_{N_x,\,j}$ for $i > N_x$ and $j = 1, \ldots, N_y$.

At the first time level, $n = 1$, initialize $G^1_{N_x+1,\,j;\,N_x,\,j_0} = \sigma^x_j \delta_{j_0,j}$. Using translation invariance in x for $x > x_{N_x}$, we can apply recursion to determine

$$G^n_{N_x+2,\,j;\,N_x,\,j_0} = \sum_{m=1}^{n-1} \sum_{k=1}^{N_y} G^m_{N_x+1,\,j;\,N_x,\,k} G^{n-m}_{N_x+1,\,k;\,N_x,\,j_0}, \quad n > 1. \tag{16}$$

The discrete wave equation produces

$$\begin{aligned} G^n_{N_x+1,\,j;\,N_x,\,j_0} \;=\; & 2G^{n-1}_{N_x+1,\,j;\,N_x,\,j_0} - G^{n-2}_{N_x+1,\,j;\,N_x,\,j_0} + \sigma^x_j \left(G^{n-1}_{N_x+2,\,j;\,N_x,\,j_0} - 2G^{n-1}_{N_x+1,\,j;\,N_x,\,j_0} \right) \\ & + \sigma^y_j \left(G^{n-1}_{N_x+1,\,j+1;\,N_x,\,j_0} - 2G^{n-1}_{N_x+1,\,j;\,N_x,\,j_0} + G^{n-1}_{N_x+1,\,j-1;\,N_x,\,j_0} \right). \end{aligned} \tag{17}$$

Note that the boundary conditions at $j = 1$, dealing with $y_{\min}$, and $j = N_y$ for $y_{\max}$ will produce slightly different results than given here for the last term on the right-hand side, which represents the second spatial derivative in y.

Figure 3(a) shows a simple but nontrivial wave speed model on which the method was tested. The domain $[0, 1] \times [0, 0.4]$ was discretized by 250×100 points and spacings $\Delta x = \Delta y = 0.004$. A point

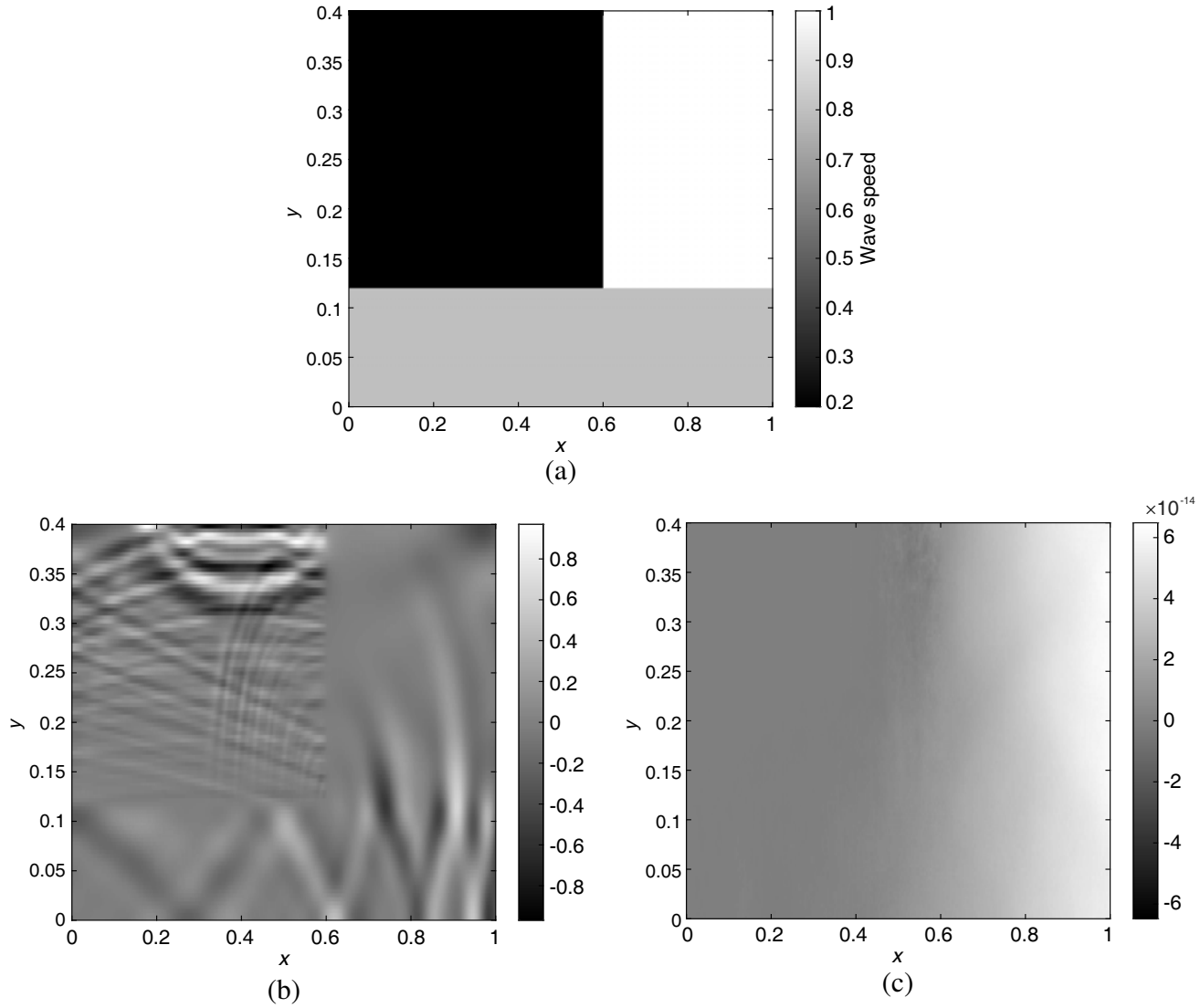

Figure 3. (a) Wave speed model. (b) Wavefield at time 2 for a point source. The Neumann boundary conditions at the left, top and bottom generate symmetric reflections. The boundary at the right is perfect. (c) Difference with a run on an enlarged domain.

source was placed at $x_s = 0.4$ and $y_s = 0.1$. Its spatial part is a delta function mimicked by an amplitude $1/(\Delta x \Delta y)$ on one grid point. The temporal source signal was $-\frac{\mathrm{d}}{\mathrm{d}t}[4(t/T_w)(1-t/T_w)]^{p_w}$ if $t \in [0, T_w]$ and zero otherwise, with a power $p_w = 12$ and duration $T_w = 0.261$. The time stepping scheme ran up to $t_{\max} = 2$, with a time step at 80% of the stability limit. Figure 3(b) shows the wavefield at time $t_{\max}$. The difference between a run with the exact non-reflecting boundary conditions and one an enlarged domain is displayed in Figure 3(c) and is dominated by numerical round-off errors.

2.6. 2D with Corners

The generalization of the above to a boundary at one side in 3D is straightforward. The same is true for an additional boundary at the opposite side, at $x = x_{\min}$. Non-reflecting boundaries at more sides, however, pose a problem. Consider, for instance, a problem with such boundaries all around the domain. If the domain is enlarged, waves entering into the exterior, the extended part of the domain, may travel around a corner, and even around more than once. A generalization of the expressions in Eq. (14)

or (15) remains valid. Unit spikes can be put next to the boundary in the original domain and their response can be recorded in the enlarged domain just outside the boundary, while the interior values are kept at zero. To keep the notation simple, we use a single flat index j_{int} for the points just inside the boundary. This involves unit spikes at $N_s = 2(N_x + N_y)$ interior points, namely, $(1, j)$ and (N_x, j) for $j = 1, \ldots, N_y$ and $(i, 1)$ and (i, N_y) for $i = 1, \ldots, N_x$. Let these be enumerated by j_{int}. For each of those, a simulation on an enlarged domain can produce $g^n_{j_{\text{int}}, j_{\text{ext}}}$ by recording values at points indexed by j_{ext}. These involve $(0, j)$ and $(N_x + 1, j)$ for $j = 1, \ldots, N_y$ and $(i, 0)$ and $(i, N_y + 1)$ for $i = 1, \ldots, N_x$. Then, a simulation on a different problem can have exact non-reflecting boundary conditions by using

$$u^n_{j_{\text{ext}}} = \sum_{m=1}^{n} \sum_{j_{\text{int}}=1}^{N_j} g^m_{j_{\text{ext}},\, j_{\text{int}}} u^{n-m}_{j_{\text{int}}}. \tag{18}$$

Unfortunately, it is not clear how to construct a recursion formula for $g^m_{j_{\text{ext}},\, j_{\text{int}}}$ because translation invariance is lost in the presence of corners.

A workaround consists in combining the numerically exact boundary condition with a classic one, for instance, the Enquist-Majda [13] or Higdon boundary conditions [2, 14, 19]. In that way, exactness is lost but the result may still be better than with solely the classic conditions, as will be discussed elsewhere [20].

2.7. Complexity

Although the proposed method is exact, it is not cheap. Here, its computational cost is estimated. In d dimensions, the grid has $O(N^d)$ points, where there are $O(N)$ number of points per coordinate direction. The time-stepping stability requires $O(N)$ time steps, resulting in an overall cost of $O(N^{d+1})$. With $O(N^{d-1})$ boundary points, a direct computation of the response functions G on an enlarged domain requires $O(N^{2d})$ operations. The recursion approach, as in Equation (17), involves G, which has a size of $O(N^{d-1})O(N_t) = O(N^d)$. Each entry costs the same amount of operations, leading to a complexity of $O(N^{2d})$, which is rather high in 2D and especially 3D. The evaluation of the discrete PDE as in (16) has negligible $O(N^{d-1})$ cost.

Table 1. Computational complexity in d space dimensions for the various methods. The number of grid points per coordinate direction as well as the number of time steps is $O(N)$.

computation	cost
modeling	$O(N^{d+1})$
enlarged domain	$O(N^{d+1})$
g^n, directly	$O(N^{2d})$
g^n, recursion	$O(N^{2d})$

Table 1 summarizes the cost of each approach. Note that a simulation on the enlarged domain involves a much larger number of points N, but since it remains proportional to the original one, the complexity stays the same. Repeating the computation on the enlarged domain for all spikes on the boundary leads to the cost for the direct computation of g^n. Recursion results in the same complexity, but now with a smaller N.

The response functions can be reused for different problems if the grid, the time step and the wave speeds near the boundary do not change. For some applications, this may justify their high cost. Otherwise, as mentioned in the introduction, one of the classic absorbing boundary conditions in combination with a carefully tuned PML strip will be a good choice.

3. CONCLUSIONS

A numerical scheme for exact non-reflecting boundaries with the simple wave equation has been presented. Tests in 1D produce stable results with a second-order central difference approximation of the spatial second derivative and with higher-order spatial discretizations up to order 24. They only differ from simulations on an enlarged domains by accumulated numerical round-off errors.

The method requires a precomputation of the response in the exterior for unit spikes at the internal boundary. The associated recursion formulae are simple but their convolutional character make them costly. Once the responses are available, they can be applied to more than one modeling problem, as long as the grid, the time step and the wave speed close to the boundary are not changed. Apart from the precomputed response functions, the boundary values of the current simulation have to be stored for all times.

The generalization to 2D involves an additional spatial convolution over boundary values. The wave speed in the exterior beyond the boundary is assumed to be obtained by piecewise constant extrapolation in the direction perpendicular to the boundary. However, precomputation by simple recursion only works with a single non-reflecting boundary on one side or two at opposing sides of a rectangular domain. The reason is that the recursion assumes translation invariance in the exterior, which is lost as soon a corner with non-reflecting boundaries at connected sides is involved. As such, the applicability of the method is limited to, for instance, modeling waveguides — or exactness should be partially abandoned.

REFERENCES

1. Givoli, D., "Non-reflecting boundary conditions," *Journal of Computational Physics*, Vol. 94, No. 1, 1–29, 1991.
2. Mulder, W. A., "Experiments with Higdon's absorbing boundary conditions for a number of wave equations," *Computational Geosciences*, Vol. 1, No. 1, 85–108, 1997.
3. Tsynkov, S. V., "Numerical solution of problems on unbounded domains. A review," *Applied Numerical Mathematics*, Special Issue on Absorbing Boundary Conditions, Vol. 27, No. 4, 465–532, 1998.
4. Tourrette, L. and L. Halpern, *Absorbing Boundaries and Layers, Domain Decomposition Methods: Applications to Large Scale Computers*, Nova Science Publishers, Inc., 2001.
5. Givoli, D., "High-order local non-reflecting boundary conditions: A review," *Wave Motion*, Vol. 39, No. 4, 319–326, 2004.
6. Antoine, X., E. Lorin, and Q. Tang, "A friendly review of absorbing boundary conditions and perfectly matched layers for classical and relativistic quantum waves equations," *Molecular Physics*, Vol. 115, Nos. 15–16, 1861–1879, 2017.
7. Gao, Y., H. Song, J. Zhang, and Z. Yao, "Comparison of artificial absorbing boundaries for acoustic wave equation modelling," *Exploration Geophysics*, Vol. 48, No. 1, 76–93, 2017.
8. Berenger, J.-P., "A perfectly matched layer for the absorption of electromagnetic waves," *Journal of Computational Physics*, Vol. 114, No. 2, 185–200, 1994.
9. Mulder, W. A. and B. Hak, "An ambiguity in attenuation scattering imaging," *Geophysical Journal International*, Vol. 178, No. 3, 1614–1624, 2009.
10. Ting, L. and M. J. Miksis, "Exact boundary conditions for scattering problems," *The Journal of the Acoustical Society of America*, Vol. 80, No. 6, 1825–1827, 1986.
11. Givoli, D. and D. Cohen, "Nonreflecting boundary conditions based on Kirchhoff-type formulae," *Journal of Computational Physics*, Vol. 117, No. 1, 102–113, 1995.
12. Teng, Z.-H., "Exact boundary condition for time-dependent wave equation based on boundary integral," *Journal of Computational Physics*, Vol. 190, No. 2, 398–418, 2003.
13. Engquist, B. and A. Majda, "Radiation boundary conditions for acoustic and elastic wave calculations," *Communications on Pure and Applied Mathematics*, Vol. 32, No. 3, 313–357, 1979.

14. Higdon, R. L., "Absorbing boundary conditions for difference approximations to the multi-dimensional wave equation," *Mathematics of Computation*, Vol. 47, No. 176, 437–459, 1986.
15. Mur, G., "Total-field absorbing boundary conditions for the time-domain electromagnetic field equations," *IEEE Transactions on Electromagnetic Compatibility*, Vol. 40, No. 2, 100–102, 1998.
16. Komatitsch, D. and R. Martin, "An unsplit convolutional perfectly matched layer improved at grazing incidence for the seismic wave equation," *Geophysics*, Vol. 72, No. 5, SM155–SM167, 2007.
17. Zhebel, E., S. Minisini, A. Kononov, and W. A. Mulder, "A comparison of continuous mass-lumped finite elements with finite differences for 3-D wave propagation," *Geophysical Prospecting*, Vol. 62, No. 5, 1111–1125, 2014.
18. Fornberg, B., "Generation of finite difference formulas on arbitrarily spaced grids," *Mathematics of Computation*, Vol. 51, No. 184, 699–706, 1988.
19. Higdon, R. L., "Numerical absorbing boundary conditions for the wave equation," *Mathematics of Computation*, Vol. 49, No. 179, 65–90, 1987.
20. Mulder, W. A., "Working around the corner problem in numerically exact non-reflecting boundary conditions for the wave equation," *Conference Proceedings, 82nd EAGE Conference and Exhibition 2020*, Amsterdam, The Netherlands, 2020.